MADRID 2015
1-4 June 2015 | IFEMA Madrid

Tu N116 04

Joint PP-PS Inversion Without Prior Data Registration

B. Roure* (CGG), V. Souvannavong (CGG), J.P. Coulon (CGG) & D. Hampson (CGG)

SUMMARY

Standard joint AVO inversion of PP and PS seismic data rely on a registration process beforehand to align PP and PS data in a common time domain. This is a difficult step prone to error that may deteriorate the inversion results. We present a new method to jointly invert PP and PS data without prior registration by integrating the travel times as well as the amplitudes in a model-based inversion. Including the travel times brings extra constraints on the VP/VS ratio and therefore helps the inversion converge. This new method is demonstrated on a shale gas data example and shows better results than PP inversion and standard joint inversion.

Introduction

The inversion of converted PS wave seismic data jointly with PP wave seismic data sometimes gives better estimates of shear-related elastic properties and density compared to the inversion of PP data only (e.g. Barnola and Ibram, 2012). Since the reflected P and S waves travel at different velocities, standard joint inversion methods heavily rely on the quality of the registration process that aligns the data in a common time domain. Details on the registration process are given in Anderson and Lines (2008) for example. Registration is a crucial step that is prone to error as illustrated in Figure 1 with a synthetic example showing seismic traces generated using logs from a well in Western Canada for angles of incidence θ ranging from 0° to 30°.

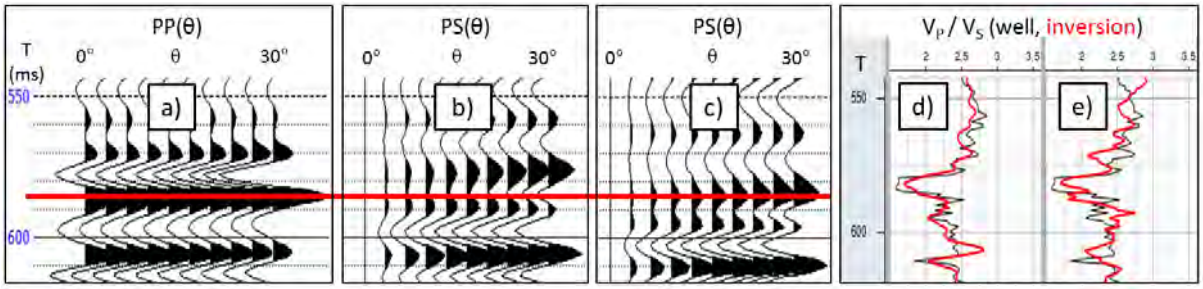

Figure 1 *Sensitivity of inversion to registration error. (a) PP seismic traces from 0° to 30°, PS seismic traces from 0° to 30° aligned to PP data (b) using correct registration and (c) using erroneous registration. d) and e) show respectively the impact of the correct and erroneous registrations on the V_P/V_S ratio estimated from joint inversion (red) together with the well logs (black).*

Figure 1b shows PS seismic traces correctly registered to the PP data (Figure 1a) using the exact velocities from the well. The red line shows that a peak on the PP data is not aligned with a peak on the PS data and an interpreter may be tempted to modify the registration to force the alignment, resulting in a new set of wrongly aligned PS traces (Figure 1c). Both datasets were then inverted using the joint inversion method described by Hampson and Russell (2013). Figures 1d and 1e show respectively the impact of the correct and erroneous registrations on the inverted P- to S-velocity ratio, V_P/V_S. The joint inversion using the wrong registration could not find an elastic response consistent with the well that matches both PP and PS seismic traces because it tries to solve for different lithologies at the same time.

Even when registration is performed correctly there are a few limitations associated with it (Anderson and Lines, 2008). The squeezing of the data associated with the registration may result in a non-stationary signal and the associated time and space variant wavelets make the inversion process unstable if they are not properly taken into account. Another limitation is that the V_P/V_S ratio volume issued from the registration is usually not incorporated into the amplitudes inversion. Furthermore the original difference in travel times between the PP and PS data is usually discarded even though it contains quantitative information that could be used in the inversion.

We present a new integrated method without prior registration that inverts jointly PP and PS data in their natural time domain and reconciles well logs data, seismic amplitudes and travel times. First we show how the reflectivity and travel time expressions of PP and PS data can be used in a model-based inversion and then we illustrate the benefits of the new approach on real data.

Method

Coulon et al. (2006) described a non-linear inversion where PP angle stacks are inverted using a simulated annealing optimization technique. This model-based inversion is defined in a stratigraphic grid which consists of layers defined in time and consistent with the geology and seismic dips. The thickness of the layers is controlled by the wavelet bandwidth. Each cell of the grid contains values describing the P-velocity, V_P, S-velocity, V_S, density, ρ, and time position of the layers, T. These properties are iteratively perturbed in order to minimize a three term cost function where the first term

measures the misfit between the real seismic amplitudes and the synthetic amplitudes calculated by 1D convolution of the reflectivities using angle-dependent wavelets. The second term of the objective function imposes lateral and vertical continuity constraints which control the smoothness of the inverted elastic properties in the presence of noise. The last term in the cost function controls how far the solution is allowed to move away from a user-specified, low-frequency initial model.
The stratigraphic inversion method can easily be extended to a joint inversion by adding PS angle stacks in PS times and their associated angle-dependent wavelets (with lower frequency than the PP wavelets). The travel time difference between PP and PS data is handled by defining two time axis in the stratigraphic grid, T_{PP} and T_{PS}, linked by the V_P/V_S ratio through the relation (Anderson and Lines, 2008):

$$\frac{V_P}{V_S} = 2\frac{\Delta T_{PS}}{\Delta T_{PP}} - 1 \tag{1}$$

where ΔT represents the thickness of the layers in PP or PS times.
The amplitudes misfit term of the cost function is modified to account simultaneously for the PP and PS data misfit in their respective time domain. The PP and PS reflectivities are computed using the Zoeppritz equations (1919) or Aki and Richards approximations (1980) whose simplified expression at an interface between two isotropic elastic media for a given angle of incidence is:

$$R_{PP} = a\frac{\Delta V_P}{\bar{V}_P} + b\frac{\Delta V_S}{\bar{V}_S} + c\frac{\Delta \rho}{\bar{\rho}} \tag{2}$$

$$R_{PS} = d\frac{\Delta V_S}{\bar{V}_S} + e\frac{\Delta \rho}{\bar{\rho}} \tag{3}$$

where Δ and $\bar{}$ are respectively the difference and the average of the properties above and below the interface, and the parameters *a*, *b*, *c*, *d* and *e* are combinations of elastic properties and angles of incidence and reflection. The benefits of including the PS reflectivity for AVO inversion are discussed in Gray (2003).
We now have a set of three equations (1-3) to invert simultaneously amplitudes and travel times. Including the travel times as part of the inversion brings extra constraints on the inverted V_P/V_S ratio. During inversion, a V_P/V_S perturbation will introduce a vertical shift in layer position in PS time. The iterative perturbation process will automatically optimize the alignment between synthetic and real data in PS time as well as the amplitudes match. This approach is similar to the handling of production-induced time-shifts in time-lapse seismic inversion (see Michou et al., 2013) where the time-shifts between vintages are used to constrain changes in V_P over time.

Shale gas example

The new joint inversion without prior registration was tested on a 2D seismic dataset of a shale gas play from Canada. Five PP and PS angle stacks are available with P-incidence angles up to 35°. Figures 2a and 2b show one of the angle stacks for PP and PS data respectively. The PS data are not registered and are depicted in native PS time domain. The red horizons correspond to the first and last layers of the stratigraphic grid in PP and PS times. They define the inversion time window. Figures 2c and 2d respectively show the inverted I_P and V_P/V_S at the vertical well located along the section. The shale reservoir interval is associated with a strong increase in V_P/V_S. Three sets of inversion results are compared in the figure: PP only inversion (green), joint PP-PS inversion with prior registration (blue) and without prior registration (red). All results are comparable in terms of I_P (or slightly worse for the PP only inversion) but show more variability in the V_P/V_S estimates. The V_P/V_S ratio from the PP inversion is consistent with the well log at the target but the contrasts above and below are underestimated, making the target more difficult to detect. The V_P/V_S ratio from the standard joint inversion is overestimated. In comparison, the new joint inversion without prior data registration provides a better fit at the target.

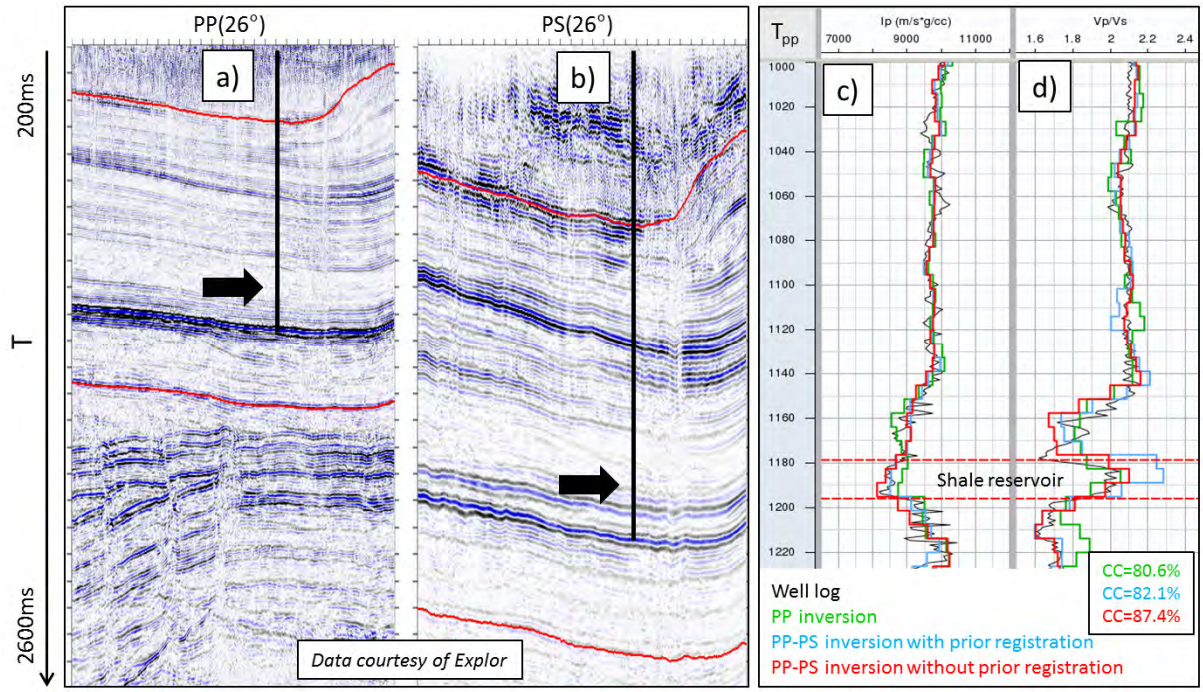

Figure 2 *(a) PP and (b) PS angle stacks displayed in PP and PS time, respectively, with red horizons corresponding to the inversion window. Arrows indicate position of shale target along vertical well. (c) I_P and (d) V_P/V_S results from different inversions are displayed together with the corresponding well logs. The correlation coefficients, CC, between the inverted V_P/V_S ratios and the well log are also displayed.*

Figure 3 illustrates how the new inversion simultaneously satisfies the amplitude and travel time information in addition to matching the well data as seen on Figure 2. Figures 3a and 3b show respectively corresponding PP and PS seismic traces extracted from the angle stacks displayed in Figure 2. Coloured markers identify the same events extracted from the stratigraphic grid in PP and PS times to illustrate the difference in travel times. Figures 3c and 3d depict the same traces after zooming, together with the corresponding synthetic traces from the PP inversion (green) and the new joint inversion (red). Both inversions show a good match to the PP seismic data in PP time (Figure 3c) but quite a different match to the PS seismic data in PS times (Figure 3d). The quality of the PP inversion can be judged by how well it predicts the PS data. The conversion to PS time in that case was done using the V_P/V_S ratio from the PP inversion. The combination of V_P, V_S and ρ estimated from the PP inversion poorly matches the PS seismic data in terms of amplitudes but also in terms of travel times. The time-shift between real and synthetic PS data reaches about 5 ms around 1575 ms and 2075 ms. In contrast, the new joint inversion provides estimates of V_P, V_S and ρ that match both amplitude and travel time simultaneously, i.e. only low PS residual amplitudes and time-shifts are observable.

Conclusions

The new joint PP-PS inversion does not require prior registration of the PS data, hence limiting the negative impact of time registration errors and registration-induced PS amplitude distortion. Travel times are included in the inversion process through the use of a stratigraphic grid, defined both in PP and PS times. Layer positions in PS time are optimized during the inversion together with the elastic properties. Including the travel times in the inversion brings extra constraints on the V_P/V_S ratio and provides better estimates compared to standard methods. Assuming all data are consistent, we reconcile information from well logs, PP amplitudes, PS amplitudes and travel time differences. The benefits of the new method were illustrated on a shale gas dataset from Canada.

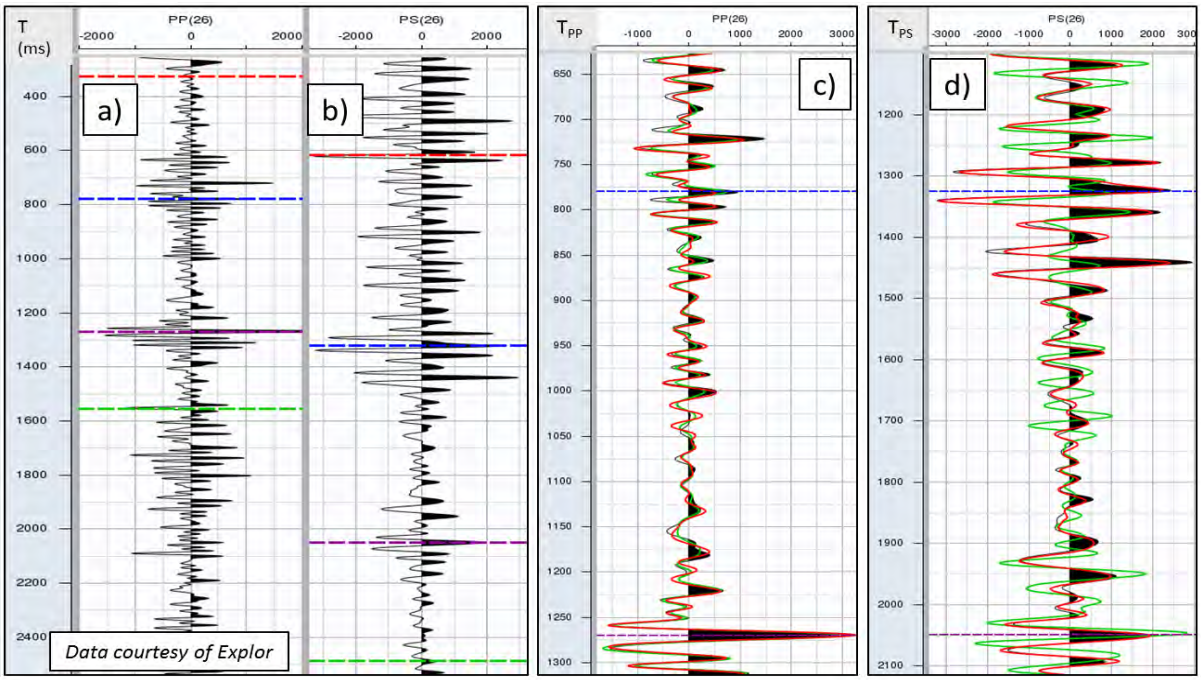

Figure 3 *Real dataset inversion results. (a) PP seismic trace and (b) PS seismic trace with different time scales visualized by coloured markers, (c) zoom on the PP seismic trace (black) in PP time together with the synthetic traces from the PP inversion (green) and joint inversion (red), (d) zoom on the PS seismic trace (black) in PS time together with the synthetic traces from the PP inversion (green) and joint inversion (red).*

Acknowledgements

The authors would like to thank Philippe Doyen and Dave Tam for their contribution and Explor for permission to show the real data example.

References

Anderson, P.F. and Lines, L.R. [2008] A comparison of inversion techniques for estimating V_P/V_S from 3D seismic data. *CREWES Research Report*, **20**.

Aki, K. and Richards, P.G. [1980] *Quantitative Seismology, 2nd edition*. University Science Books.

Barnola, A.-S. and Ibram, M. [2012] 3D Simultaneous Joint PP-PS AVO Seismic Inversion in Schiehallion Field, UKCS. *74th EAGE Conference and Exhibition*, Extended Abstract, C003.

Coulon, J.-P., Lafet, Y., Deschizeaux, B., Doyen, P. M. and Duboz, P. [2006] Stratigraphic elastic inversion for seismic lithology discrimination in a turbiditic reservoir. *SEG Expanded Abstracts*, 2092-2096.

Gray, F.D. [2003] P-S Converted-Wave AVO. *SEG Expanded Abstracts*, 165-168.

Hampson, D. and Russell, B. [2013] Joint simultaneous inversion of PP and PS angle gathers. *CSEG Recorder*, **38**(6), 32-39.

Michou, L., Coleou, T., Lafet, Y. and Roure, B. [2013] 4D Seismic Inversion on Continuous Land Seismic Reservoir Monitoring of Thermal EOR. *GeoConvention*, Extended Abstracts.

Zoeppritz, K. [1919] Erdbebenwellen VIII B, Über die Reflexion und Durchgang seismischer Wellen durch Unstetigkeitsflächen. *Gottinger Nachr. 1*, 66-84.